

<https://doi.org/10.1038/s43247-024-01902-w>

# Arctic plant-fungus interaction networks show major rewiring with environmental variation

Check for updates

Bastien Parisy <sup>1</sup>✉, Niels M. Schmidt <sup>2,3</sup>, Alyssa R. Cirtwill <sup>1,4</sup>, Edith Villa-Galaviz <sup>5</sup>, Mikko Tiusanen <sup>6</sup>, Cornelya F. C. Klütsch <sup>7</sup>, Paul E. Aspholm <sup>7</sup>, Katrine Raundrup <sup>8</sup>, Eero J. Vesterinen <sup>9</sup>, Helena Wirta <sup>1,10</sup> & Tomas Roslin <sup>11,12</sup>

Global environmental change may lead to changes in community structure and in species interactions, ultimately changing ecosystem functioning. Focusing on spatial variation in fungus–plant interactions across the rapidly changing Arctic, we quantified variation in the identity of interaction partners. We then related interaction turnover to variation in the bioclimatic environment by combining network analyses with general dissimilarity modelling. Overall, we found species associations to be highly plastic, with major rewiring among interaction partners across variable environmental conditions. Of this turnover, a major part was attributed to specific environmental properties which are likely to change with progressing climate change. Our findings suggest that the current structure of plant–root associated interactions may be severely altered by rapidly advancing global warming. Nonetheless, flexibility in partner choice may contribute to the resilience of the system.

Species interactions are the key process underlying ecosystem functions and services. In terrestrial ecosystems, interactions between plants and soil microorganisms, such as fungi, are particularly important for functions including nutrient cycling and carbon storage<sup>1</sup>. Understanding how climate change affects the networks of such interactions in a community is thus key to understanding the consequences of environmental change for ecosystem functioning<sup>2</sup>.

Ecological networks can change in two main ways: through changes in the set of co-occurring species (nodes) and through changes in interactions (links) among co-occurring species<sup>3</sup> (Fig. 1). The latter phenomenon is referred to as “rewiring”<sup>3</sup>. As these two types of changes come with different consequences for network stability and robustness<sup>4,5</sup>, ecologists have recently tried to formally quantify the two<sup>3,6</sup>. Flexibility in links has been shown to add to the robustness of interaction networks – since if one interaction partner disappears, then species can compensate by forming alternative interactions with other partners of similar function (adding to functional redundancy)<sup>4,5</sup>. Thus, different levels of rewiring will result in different levels of secondary extinctions among dependent species<sup>4,7,8</sup>.

Cases of major rewiring have recently been reported from local studies of plant–microbe interactions of peatland ecosystems<sup>9</sup>, and in plant–pollinator networks<sup>10–12</sup>. Yet, to what extent these reports represent isolated findings, or a general rule, is still to be determined. Of particular interest is how rewiring is driven by environmental conditions, and thus susceptible to global change.

In this study, we empirically quantified changes in plant–fungus networks with geographic and environmental variation across the Arctic, assessing the degree to which plants and fungi show consistent associations. By targeting interactions as such, we build further from studies focusing on compositional turnover among fungi and plants on their own (Fig. 1A, top). Such variation has been extensively studied, suggesting that the diversity and species composition of plant communities is mainly determined by temperature and by edaphic conditions<sup>13–16</sup> (i.e., pH, nutrients and moisture). By comparison, turnover in fungal communities of the Arctic appears to be driven by turnover in the community of plants, with additional imprints of environmental conditions<sup>17</sup>. Thus, the determinants of community composition may differ from the determinants of interaction composition

<sup>1</sup>Department of Agricultural Sciences, Faculty of Agriculture and Forestry, University of Helsinki, Helsinki, Finland. <sup>2</sup>Department of Ecoscience, Aarhus University, Roskilde, Denmark. <sup>3</sup>Arctic Research Centre, Aarhus University, Roskilde, Denmark. <sup>4</sup>Carex EcoLogics, Bracebridge, Canada. <sup>5</sup>Ecological Networks lab, Department of Biology, Technical University of Darmstadt, Darmstadt, Germany. <sup>6</sup>Department of Environmental Systems Science, ETH Zürich, Zürich, Switzerland. <sup>7</sup>Norwegian Institute of Bioeconomy Research (NIBIO), Department of Ecosystems in the Barents Region, Svanvik, Norway. <sup>8</sup>Greenland Institute of Natural Resources, Nuuk, Greenland. <sup>9</sup>Department of Biology, University of Turku, Turku, Finland. <sup>10</sup>Department of Ecology and Environmental Science, Umeå University, Umeå, Sweden. <sup>11</sup>Department of Ecology, Swedish University of Agricultural Sciences, Uppsala, Sweden. <sup>12</sup>Organismal and Evolutionary Biology Research Programme, Faculty of Biological and Environmental Sciences, University of Helsinki, Helsinki, Finland. ✉e-mail: [bastien.parisy@helsinki.fi](mailto:bastien.parisy@helsinki.fi)

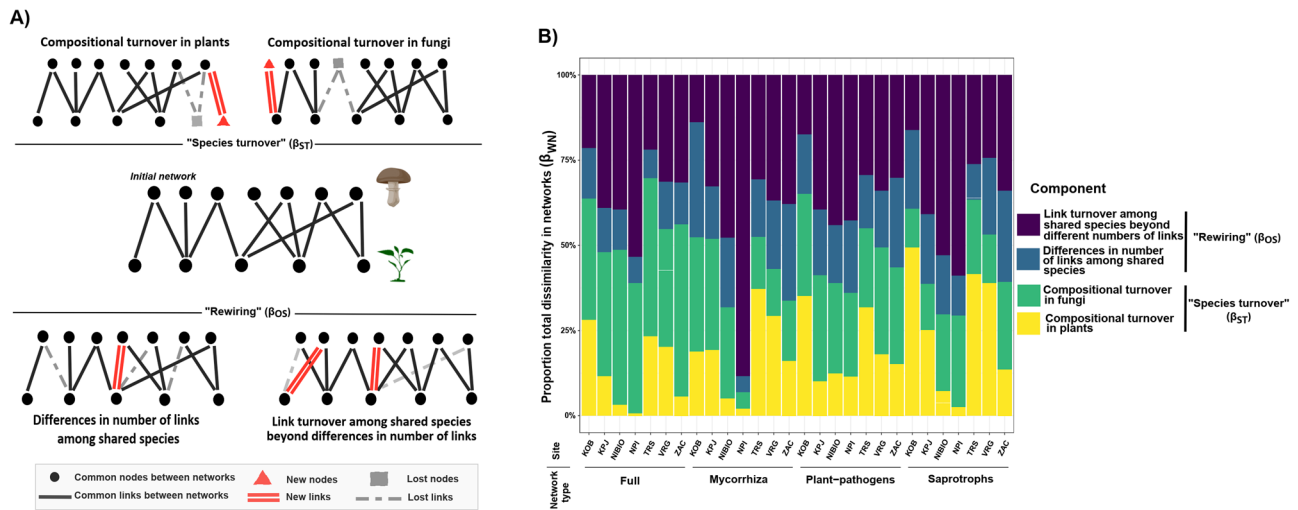


**Fig. 1 | Components of variation in the link structure of ecological networks and their empirically-quantified contribution to link variation across the Arctic.**

Panel (A) illustrates how a hypothetical initial plant–fungus network (central network) can be altered by four mechanisms: (1) By changes in the composition of the plant community (i.e., by links being lost or new links being formed through the loss or gain of plant species; top-left network); (2) by changes in the composition of the fungal community, (i.e., by links being lost or new links being formed through the loss or gain of fungal species; top-right network); (3) by changes in the number of links between resident species (bottom-left network); and (4) by changes in link identity without changes in link numbers among resident species (bottom-right network). Red triangles represent new nodes added to the network; grey squares represent nodes disappearing from the network; and black circles represent nodes shared between networks. Links preserved in the network are shown by black filled lines, disappearing ones by grey dashed lines and new links by red double lines. Panel

(B) shows the partitioning of overall variation in network structure observed across the Arctic into the components defined in (A). Here, we partition total variation in link structure observed across regional sub-networks ( $\beta_{WN}$ ) into the components defined in (A). Fractions along the x-axis show the same partitioning applied first to the full set of all fungi associated with plant roots (“FULL”) and then to three subnetworks consisting of plants and individual groups of fungi defined by their type of interaction with the plant: plants vs. mycorrhizal fungi (“Mycorrhiza”), plants vs. pathogenic fungi (“Plant-pathogens”) and plants vs. saprotrophic fungi (“Saprotrophs”), respectively. Labels along the x-axis identify individual arctic sites: KOB= Kobbefjord, South-West Greenland; KPJ = Kilpisjärvi, Finland; NIBIO = Gandvik valley, Norway; NPI = Ny Alesund, Svalbard; TRS = Toolik Research Station, Alaska; VRG = Varanger Peninsula, Norway, ZAC = Zackenberg, North-East Greenland (for a map of these sites, see Supplementary Fig. 1).

(Fig. 1A, middle)<sup>18,19</sup>. To understand overall variation in species interactions, we should adopt a new framework separating turnover in species composition from turnover in the links between co-occurring species (Fig. 1, all panels combined).

To partition overall turnover in network structure into turnover caused by changes in the identity of the nodes and changes in links among co-occurring nodes, we adopted the seminal framework of Poisot et al.<sup>18</sup> (Fig. 1). In brief, variation in link structure can occur through the loss or gain of links between resident species, or through the loss of previous species or the gain of new species (Fig. 1). Thus, we followed Noreika et al.<sup>11</sup> in quantifying four different contributions to overall variation in the links observed at each site (Fig. 1A): (1) changes in networks caused by compositional turnover of the fungal community (i.e., links lost or new links formed by the loss or gain of fungal species; (2) compositional turnover of the plant community; (3) changes in the number of links between resident species; and (4) changes in link identity without changes in link number among resident species.

Given a major imprint of abiotic conditions on species composition in arctic communities<sup>20</sup>, we a priori expected changes in plant–fungal networks to be driven by species turnover rather than by rewiring of interactions. Within networks, we expected higher host specificity in plant–mycorrhizal and/or plant–pathogen networks than in saprotroph–fungus networks, since the former interact with living plant tissue, but the latter with decaying organic matter<sup>21</sup>. Thus, pathogens will strongly respond to the ecophysiological traits of plants (including their immune system), whereas saprotrophs may be less affected by specific host traits—but still respond to factors such as leaf litter chemistry<sup>22,23</sup> or endophytic fungi growing in or on the host<sup>24</sup>. Higher partner-fidelity in plant–mycorrhizal and/or plant–pathogen networks should, in turn, translate into lower rewiring. Finally, since fungal communities<sup>25</sup> and plant–fungus associations<sup>26</sup> are sensitive to temperature and soil conditions, we expected a major part of variation in network structure to be attributable to these environmental features. Should this be the case in space, then can predict continuing rewiring over time, as both

temperature and soil conditions are expected to change under future climatic scenarios<sup>27</sup>.

To evaluate the above hypotheses, we used DNA metabarcoding of the ITS region to characterize fungal communities in the rhizosphere (i.e., fungi living in direct association with the target plant species) of target plants. Field sampling was conducted at two spatial scales across the Arctic: a pan-arctic scale and a regional scale (for full details, see Methods). To represent variation along local environmental gradients within each site, we sampled plant roots in replicate plots (Supplementary Fig. 1). Of the following twelve plant species, we sampled the five most locally abundant ones in each plot: *Saxifraga oppositifolia*; *Bistorta vivipara*; *Dryas* spp.; *Vaccinium vitis-idaea*; *Vaccinium uliginosum*; *Vaccinium myrtillus*; *Empetrum nigrum*; *Betula nana*; *Salix arctica*; *Salix polaris*; *Cassiope tetragona*; and *Silene acaulis*. To resolve the impact of interaction type on interaction specificity, these plant taxa were selected to represent different types of mycorrhizal associations (see Methods). Overall, we collected three root fragments for each of 1,450 root samples across 129 plots and a latitudinal gradient of 14.5 latitude (from 64.08° to 78.56°N).

In assessing the contribution of compositional turnover in the plant community to overall interaction turnover, we should make a note on the study design. As we consistently focused on a subset of twelve plant taxa, of which we sampled the five most locally abundant species (Supplementary Fig. 1), compositional turnover in plants was only weakly reflective of the underlying ecological drivers: ecological conditions will only affect the occurrence and abundance of plants within the predefined set of twelve taxa. Had we sampled a smaller set of plants, or the full vegetation, then compositional turnover among plants would per necessity have accounted for more or less variation, respectively, than currently found. As a consequence, this quantity was mostly determined by the researchers, and its size is of little interest in itself. Yet, we still quantify it and report it in our results, to prevent it from inflating the other variance components which are of primary interest.

To pinpoint the drivers of turnover in plant–fungus interactions along environmental gradients, we used Generalized Dissimilarity Models (GDMs<sup>28</sup>). Here, we focused on the two major components of dissimilarity in link structure to their environmental drivers: differences due to the turnover of nodes (i.e., “species turnover”;  $\beta_{ST}$ ), and differences in links among co-occurring species (“rewiring”;  $\beta_{OS}$ ) (Fig. 1A). Of these, the former is a standard application of GDMs, whereas the latter offers a novel application of GDMs.

## Results and discussion

### Plant–fungus interactions show major rewiring across the Arctic

None of our initial expectations was supported by the results. Rewiring of interactions between shared species contributed as much to variation in network structure as did compositional turnover of species. Overall, the rewiring ( $\beta_{OS}$ ; Fig. 1) accounted for 51% of all variation in full network structure (i.e., networks including all types of fungi) across sites (Fig. 1B). The substantial rewiring observed occurred against a backdrop of major turnover in species ( $\beta_{ST}$ ) accounting for 49% of all variation in link structure (Fig. 1B). On average, link turnover among shared species (Fig. 1A) accounted for 40% of all differences in network structure among the full set of plant–fungi networks, whereas compositional turnover among fungi contributed an average of 36% of all variation in link structure (Fig. 1B). The same patterns emerged regardless of whether we examined the network as a whole or as split into smaller networks corresponding to functional guilds (Fig. 1B). However, plant–mycorrhizal networks exhibited the highest link turnover among shared species, explaining 50% of the variation of these networks, with a maximum of 90% observed at our northernmost site (NPI; Fig. 1B). In comparison, only 19% (on average) of variation in links between plants and associated mycorrhiza was attributed to compositional turnover among fungi (Fig. 1B).

To evaluate whether the turnover observed could be attributed to random resampling from the same overall network, we compared the observed pattern to those expected if samples of the current size had been drawn from a single, site-level metaweb (i.e., from the aggregated network of all observed interactions across plots within sites). In generating these random realizations, we used the metaweb to draw networks equal in size and connectance (i.e., total number of links) to the original plot-specific networks. We then used a *z*-score to compare the deviation between the observed and expected value of each  $\beta$ -diversity component to the standard deviation of pairwise similarities across 1000 random draws from the metaweb<sup>19</sup>. Here, link turnover among species shared among sites proved consistently stronger than expected by chance (Supplementary Text 1; Supplementary Fig. 2). By comparison, compositional turnover among fungi was not significantly bigger than expected by chance alone, and thus consistent with random resampling from a shared pool of fungal species across plots within sites.

Taken together, all our data reveal that plants and fungi frequently change interaction partners even when co-occurring in the same plot, regardless of the functional role assumed by the fungi. While contradicting our initial expectation, this result is in line with a previous finding<sup>9</sup> of major turnover in link structure in the plant–microbe interactions of peatland ecosystems. It also matches findings from other types of ecological networks, such as plant–pollinator interactions<sup>10–12</sup>, where strong link rewiring has been found across site-specific networks.

### Environmental conditions dictate species composition but not link structure

Environmental conditions influenced variation in species composition—but not in link structure. Across our sub-networks, GDMs resolved a consistent, major effect of environmental conditions on the turnover of nodes ( $\beta_{ST}$ ; Fig. 2), but not on the rewiring of co-occurring taxa ( $\beta_{OS}$ ; Fig. 2). Despite some local context-dependency (Supplementary Table 1), a major proportion of the overall dissimilarity in networks and of the turnover of nodes was explained by abiotic conditions (57% of  $\beta_{WN}$ , 39% of  $\beta_{ST}$  on average; Fig. 2). Overall, temperature, edaphic conditions (especially pH),

and vegetation cover appeared more important drivers of networks structure than did carbon and nitrogen content—or geographic distance—in structuring plant–fungus associations (Supplementary Fig. 3).

Importantly, temperature and vegetation cover are far from independent of each other—as also revealed by the substantial proportion of variation shared between these factors (Fig. 2). Given our study design, these patterns will clearly concern variation in space, but may also suggest changes in plant–fungus networks over time. While we must be careful in inferring or predicting trends in time from patterns in space<sup>29,30</sup> increasing temperatures are currently driving similar, linked changes in vegetation phenology, abundance and composition<sup>31</sup> and in edaphic conditions<sup>32</sup>, resulting in a general “greening of the Arctic”<sup>31</sup>. All these factors may thus change in concert in both space and time, and thus exert a joint effect on the networks through both direct and indirect effects (cf. Fig. 2).

The effects of environmental conditions on species composition are likely attributable to local environmental filtering, where local conditions select for specific fungi and for specific interactions. Previous studies have shown that at finer spatial scales, fungal communities associated with plant roots can exhibit habitat specificity related to local temperature or edaphic conditions<sup>33</sup>. Consistent with these findings, our results suggest that temperature and abiotic soil conditions, primarily pH, did structure the overall communities. In other words, niche differentiation among interaction partners (nodes) is strongly modulated by local temperature and edaphic conditions, and thus relatively predictable.

In contrast, environmental conditions explained, on average, only 9% of the rewiring ( $\beta_{OS}$ ; Fig. 2). Some of this variation may be due to local abundance variation left unresolved by the current study design. Indeed, it has been shown that species can switch partners in response to changing abundances, even if their interaction partners are still present<sup>34</sup>. Moreover, while our study covered the main part of root-associated fungal diversity, it failed to account for the impact of other taxa. Organisms such as bacteria and invertebrates may affect interactions between plant and fungi<sup>35,36</sup>, but were here unresolved. How much they contributed to local variation in plant–fungus interactions will thus remain unknown.

Nonetheless, our general results are in line with previous studies targeting plant–pollinator interactions. Here, community dissimilarity has been found to be highly predictable along environmental gradients, whereas interaction dissimilarity is poorly explained by the environment<sup>19,37</sup>. Together, these findings imply that most variation in *which specific links* are formed at a particular site remained unexplained. This level of plasticity observed in link formation across sites supports the notion that interactions are probabilistic rather than deterministic in nature<sup>38,39</sup>, with considerable random variation in site-specific outcomes. Consequently, our study depicts local interaction networks among plant and associated fungi not as deterministic submatrices cut out of a fixed metaweb, but rather as stochastic samples, where environmental conditions mould local interaction probabilities.

### All functional guilds show plasticity in partner choice

Overall, our study reveals pronounced rewiring of the full plant–fungi networks among sites—with no real differences between different functional guilds (Fig. 1). This pattern is at odds with our initial prediction of higher host specificity in plant–mycorrhizal and/or plant–pathogen networks, and of such partner-fidelity reflecting into lower rewiring. Instead, rewiring proved equally high in all sub-networks (for an in-depth analysis of partner fidelity in different parts of the network, see Parisy et al.<sup>40</sup>).

These non-random patterns support the recent suggestion by Toju et al.<sup>41</sup> that the architecture of plant–fungus networks is fundamentally flexible, with plasticity in partner choice extending equally to mutualistic and antagonistic interactions. Local adjustments may then reflect adaptive interaction rewiring<sup>42</sup>: in harsh arctic environments, fungi may preferentially associate with any available partner rather than being associated with no partner at all<sup>43</sup>. In making this sweeping suggestion, we should hurry to add an important caveat: *some* fungi in the Arctic region may still be more

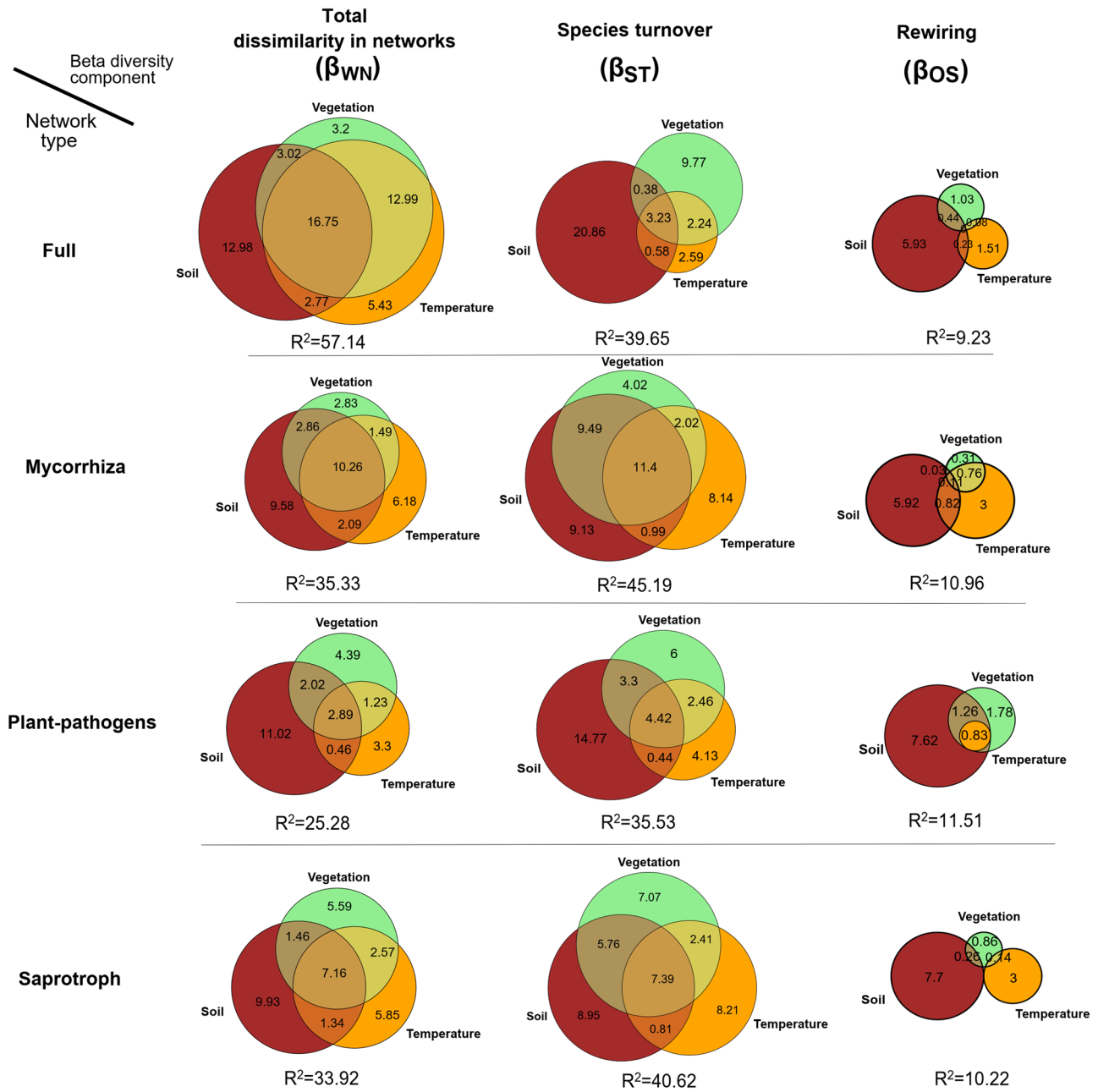


**Fig. 2 | Partitioning of model deviance for beta diversity between sub-networks.** Depicted are the deviance components of total dissimilarity of networks ( $\beta_{WN}$ ), in links ( $\beta_{OS}$ ) and in nodes ( $\beta_{ST}$ ) attributed to edaphic conditions (brown), temperature (orange), and vegetation coverage (green) variables. See Materials and Methods for further details. The Euler diagrams show the unique and shared contribution of each variable. Values represent component-specific average percentages of deviance explained across our seven sites.  $R^2$  refers to the average deviance explained by our

models, with the overall size of each Euler diagram proportional to overall  $R^2$ . “Network types” refer to different subsets of the same networks: to the full set of all fungi associated with plant roots (“FULL”) and to three subnetworks consisting of plants and individual groups of fungi defined by their type of interaction with the plant: plants vs. mycorrhizal fungi (“Mycorrhiza”), plants vs. pathogenic fungi (“Plant-pathogens”) and plants vs. saprotrophic fungi (“Saprotrophs”), respectively.

selective than others. Our study did not, for example, resolve communities of arbuscular mycorrhiza or endophytic fungi—some of which are known to be highly host specific<sup>24,44,45</sup>.

Altogether, our study indicates that an interaction between plant and fungi (regardless of their function) does not necessarily occur whenever two species that *can* interact meet, but that the probability of interaction will vary with the environment. Ultimately, the set of interactions occurring at a given time in a given place may be moulded by both abiotic and biotic impacts on link probability<sup>39,46</sup>. To understand and predict ecological networks in a changing environment, it is thus imperative to separate between impacts on species pools and link structure.

## Conclusion

To the best of our knowledge, our study is the first to explore how the beta diversity components of the plant–fungus networks vary along environmental gradients across the Arctic—or anywhere else. Here, our application of General Dissimilarity Modelling to networks in general and link structure in particular adds an important tool. Altogether, high levels of link plasticity and strong imprints of environmental conditions on link formation suggest that arctic plant–fungus networks will be strongly moulded by progressing climate change. Exactly how the resulting rewiring will affect plant fitness and the dynamics of plant communities should next be



established. Importantly, the formation of new pairs of fungi and plants may affect the performance of both components<sup>5</sup>. At the same time, overall plasticity in link structure may add to the resilience of networks in general<sup>41,47</sup>. Thus, to resolve the knock-on effects of the patterns observed, our spatial snapshot of contemporary networks across the Arctic should be urgently supplemented by temporal datasets covering both species and networks over time<sup>48</sup>. Identifying how rewiring may alter the robustness or stability of networks and the services that they provide emerges as a key task for studies to come.

## Material and methods

### Sample collection

To evaluate the impact of community assembly processes across multiple spatial scales, we used a part of an existing dataset collected and described in Parisy et al.<sup>40</sup>. We coordinated field sampling at two spatial scales: a pan-arctic scale and a regional scale. During the summers of 2020 and 2021, we collected a total of 1450 root in seven sites across a gradient of 14.5 latitude.

To characterize variation along local environmental gradients within each of our seven sites, we defined at least three local transects. These transects were located at least 250 meters apart from each other across a joint elevation gradient. To capture differences in local environmental conditions, we selected the strongest elevational gradients available in the vicinity of each site (i.e., the gradients spanning the largest difference in altitude). Within three sites (Kilpisjärvi, Varanger, and Zackenberg), we sampled more intensively following a stratified random sampling design across multiple elevational gradients.

Along each transect, we established four plots with a radius of approximately 25 m each. These plots were selected at least 100 meters from each other along the slope. A plot was selected only if at least three of the five target species occurred within the plot (no matter which species; see list below). At each site, we sampled at least 8 plots. All geographical coordinates and altitudes were recorded using a handheld GPS.

As focal plant species, we selected species common and widespread enough to be sampled across the Arctic region (Supplementary Fig. 1). Thus, within each site, the set of target species to be sampled was defined as the five most locally abundant species out of the following list: *Saxifraga oppositifolia*; *Bistorta vivipara*; *Dryas* spp.; *Vaccinium vitis-idaea*; *Vaccinium uliginosum*; *Vaccinium myrtillus*; *Empetrum nigrum*; *Betula nana*; *Salix arctica*; *Salix polaris*; *Cassiope tetragona*; and *Silene acaulis* (for the list of species collected within each site, see *Figure Materials 1 A*). Of these taxa, *Dryas* spp. represents a species complex. In North America, the dominant species is *Dryas integrifolia* and in Europe it is *Dryas octopetala*. Nonetheless, the two species interbreed, with individuals in Northeast Greenland (Zackenberg) mainly being hybrids *Dryas octopetala* × *integrifolia*<sup>49,50</sup>.

Importantly, these plant taxa were a priori selected to represent mycorrhizal types: *Betula nana*, *Bistorta vivipara*, *Dryas* spp., *Salix polaris* and *Salix arctica* have been previously assumed to be associated with ectomycorrhiza (ECM<sup>21–53</sup>); *Cassiope tetragona*, *Vaccinium myrtillus*, *Vaccinium uliginosum*, *Vaccinium vitis-idea* and *Empetrum nigrum* are mainly classified as having ericoid mycorrhiza (ErM) but are sometimes associated with ectomycorrhiza, too<sup>54–57</sup>; *Silene acaulis* and *Saxifraga oppositifolia* are generally assumed to be poorly associated with mycorrhiza, but are sometimes associated with arbuscular mycorrhiza (AM)<sup>44,53,58</sup>.

To characterize fungal communities in the rhizosphere (i.e., directly interacting with the target plant species), we collected three root fragments (length > 3 mm) from different parts of the root architecture, for 2–3 individuals of each target plant species found within the plot. To this aim, we gently dug and/or scraped 2–3 cm around the focal plant individual until we found the roots (clearly identified as connected to the stem). We then excavated the roots without breaking their fine parts and collected the soil attached to the root. The resulting sample was then considered as a compound community type: the rhizosphere. The rhizosphere was then stored within a tissue and put into a zip-lock bag filled with silica gel, which was then placed at –20 °C.

### Environmental data

As described in Parisy et al.<sup>40</sup>, to characterize the local climate, we extracted the annual mean temperature (BIO1) of each site from the WorldClim database<sup>59</sup>. We then associated the average elevation of each plot within a site with a mean annual temperature. Assuming a decline of 0.7 °C for every 100 m a.s.l., we used the mean elevation as the baseline and then subtracted or added 0.7 °C for every 100 m below or above the average, respectively. This 0.7 °C factor was defined following the standard lapse rate<sup>60</sup> and consistent with highly-resolved data collected by de la Peña-Aguilera et al.<sup>61</sup>.

Vegetation cover surrounding each focal plant individual in a 1 m<sup>2</sup> area was estimated visually. The average vegetation coverage of each plot was then calculated from all the individual estimates. For three plots at the Zackenberg site (ZAC10, 11, and 12), we lacked information on plot-level vegetation. For these plots, we used the mean of all other plots within the site as a conservative measure of vegetation coverage.

Around each targeted plant, we collected a bulk soil sample (i.e., 1450 soil samples in total) out of which we measured soil chemistry as represented by pH, carbon and nitrogen content measured at the plot level. From all the soil samples collected within each plot, we pooled soil samples collected around each target plant species sampled locally. The pooled soil was then oven-dried at 70 °C and homogenized using a sieve with a 2 mm mesh size. 0.15 mg of soil was weighted with an air-vacuumed balance, placed in tin foil, and analysed for carbon and nitrogen content using a Leco series 828 series analyser (Leco, United states). Nitrogen and carbon content was measured for each pooled soil sample using the LCRM method and calibrated with soil samples of known concentration. Another part of the pooled soil sample was used to measure pH following the ISO 10390:2021 standards (<https://standards.iteh.ai/>). For this, we prepared a 1:5 (volume fraction) suspension of soil with water, shook the suspension for 60 min using a mechanical shaker and left it to rest at least 1 h before measurement. The pH probe was calibrated with three buffers of pH 4.00, 6.88, and 9.22, respectively.

### DNA metabarcoding

As described in Parisy et al.<sup>40</sup>, The whole rhizosphere samples were used for the laboratory analysis, implemented by Bioname Ltd. ([www.bioname.fi](http://www.bioname.fi)) as a turnkey service from sample handling through bioinformatics to final data as taxa × sample matrices.

The rhizosphere samples were first cut into small pieces using DNA-clean scissors, and then homogenized together with ceramic 2 mm beads in sterile 50 ml Falcon tube for 10 min in a Bullet Blender 50DX (Next Advance, Inc., Troy, NY, USA). DNA was extracted following the protocol of Vesterinen et al.<sup>62</sup>, with some modifications as follows: A fixed volume (30 ml) of pre-warmed 60 °C lysis buffer<sup>62,63</sup> and 30 µL of proteinase K were added to the sample, and the mix was incubated for exactly 2 h 45 min at +60 °C in a shaking incubator. After incubation, 200 µL of the lysate was transferred to the next step, and excess lysate was stored in a clean 50 ml tube in –20 °C. To purify the DNA, 200 µL of the lysate was mixed with 400 µL in-house SPRI bead solution<sup>62</sup> and purified using an Opentrons OT-2 automated liquid-handling robot (New York, USA). During the robotic steps, the DNA was bound to the SPRI beads, drawn to the magnet, and the supernatant was discarded. Then, the DNA pellet was washed twice using 40 µL freshly prepared 80% ethanol. After removing all ethanol, the pellet was dried, and DNA was eluted to 200 µL of pure RNase, DNase-free water. A DNA extraction control was added to each extraction batch, containing all the reagents, except the sample material. DNA purity and integrity were assessed by PCR success rate.

The fungal ITS gene region was amplified by using primer pair tagF-ITS7 (5'-GTGARTCATCGAATCTTTG-3'<sup>64</sup>) and tagR-ITS4 (5'-TCCTCCGCTTATTGATATGC-3'<sup>65</sup>). This primer pair is designed to amplify fungi over plants<sup>66</sup>. All the primers included a linker-tag, enabling the subsequent attachment of NGS adapters. To increase the diversity of the amplicon library, each primer was used as two different versions, as including so-called heterogeneity spacers between the linker-tag and the actual locus-specific oligo. All PCR reactions were carried out as two

technical replicates, and each replicate contained two heterogeneity versions of each primer. The reaction setup followed Kankaanpää et al.<sup>67</sup>, and included 5 µL of 2× MyTaq HS Red Mix (Bioline, UK), 2.4 µL of H<sub>2</sub>O, 150 nM of each primer (two forward and two reverse primer versions), and 2 µL of DNA extract per each sample in 10 µL total-volume. A blank PCR control was added to each PCR batch to measure the purity of reagents and the level of cross-contamination. PCR was performed under the following cycling conditions: 3 min in 95 °C, then 35 cycles of 20 s in 95 °C, 30 sec in 55 °C and 20 s in 72 °C, ending with 7 min in 72 °C.

Library preparation followed Vesterinen et al.<sup>62</sup>, with minor modifications as follows: a dual indexing strategy was used, where each reaction (including technical replicates) was prepared with a unique combination of forward and reverse indices. All index sets were perfectly balanced so that each nucleotide position included either T/G or A/C, as this ensures base calling for each channel in the sequencing. For a reaction volume of 10 microliters, we mixed 5 µL of MyTaq HS RedMix, 500 nM of each tagged and indexed primer (i7 and i5) and 3 µL of the locus-specific PCR product from the first PCR. For library preparation PCR, the following protocol was used: initial denaturation for 3 min at 98 °C, then 12 cycles of 20 s at 95 °C, 15 s at 60 °C and 30 s at 72 °C, followed by 3 min at 72 °C. All the indexed samples were then pooled and purified using magnetic beads<sup>68</sup>. Sequencing was done on an Illumina NovaSeq6000 SP Flowcell 2 × 250 (Illumina Inc., San Diego, California, USA) run, including PhiX control library by the Turku Centre for Biotechnology, Turku, Finland.

The bioinformatics pipeline closely followed Kaunisto et al.<sup>69</sup>. Paired-end reads were merged and trimmed for quality using 64-bit VSEARCH version 2.14.2<sup>70</sup>. The primers were removed from the merged reads using software CUTADAPT version 2.7<sup>71</sup>, with a 20% rate for primer mismatches and 100 bp minimum length. The reads were then collapsed into unique sequences (singletons removed) with command 'fastx\_uniques' using VSEARCH. Unique reads were denoised (i.e., chimeras were removed) and reads were clustered into ZOTUs ("ZOTU" = zero-radius operational taxonomic unit) with command 'unoise3' using 32-bit USEARCH version 11<sup>72</sup>. All samples with fewer than 50 reads in total were removed, and all ZOTUs from a sample with less than 20 reads for that ZOTU or with less than 0.05% of the total read number (all reads assigned to ZOTUs) of that sample were removed. Finally, ZOTUs were assigned to taxa by using the UNITE database<sup>73</sup> with SINTAX<sup>72</sup> in VSEARCH<sup>70</sup>. All ZOTUS with under 97% similarity to any reference database sequence were discarded. Finally, ZOTUS were assigned to a functional group by using the FUNGUILD python script (<https://github.com/UMNFuN/FUNGuild> <https://github.com/UMNFuN/FUNGuild>), which matches taxonomic assignment at genus level against the FUNGuild database<sup>74</sup>. Out of the 459 fungal genera detected, 278 were assigned to a functional group (60.6%).

### Statistical analyses: How do the components of plant–fungus networks change across environments?

All analyses presented below were performed in R (version 4.4.1). Overall differences in networks between sites ( $\beta$ -diversity) are essentially made up of two components: turnover in species and turnover in links (Fig. 1). The later element can be further partitioned into two components: links not realized because the two nodes do not co-occur, and to rewiring (i.e., differences in links between species which do co-occur<sup>18</sup>, Fig. 1). To evaluate the contributions of these different components to the patterns resolved above, the  $\beta$ -diversity of subnetworks (i.e., plot-scale networks), by comparing the number of shared and unique links among species within a pair of networks.

Following Poisot et al.<sup>18</sup>, we measured variation in network structure using the Sorensen dissimilarity index, in which interaction dissimilarity is calculated between two networks M and N as  $\beta_{WN} = (b + c)/(2a + b + c)$ , wherein  $a$  is the number of interactions occurring in both networks,  $b$  is the number of interactions occurring only in the network M, and  $c$  is the number of interactions occurring only in the network N<sup>3</sup>. Furthermore, the  $\beta$ -diversity of networks can be partitioned into the dissimilarity due to difference in species composition (i.e., species turnover " $\beta_{ST}$ ") and

dissimilarity due to interaction rewiring (i.e., flexibility of interactions among shared species " $\beta_{OS}$ ") which is equal to  $\beta_{WN} = \beta_{ST} + \beta_{OS}$ <sup>3,18</sup>.

To date, numerous variations of  $\beta$ -diversity metrics have been proposed, with little consensus regarding which measure is most appropriate in a given situation<sup>3,6</sup>. In the current study, we used an approach initially proposed by Novotny et al.<sup>75</sup> and further refined by Legendre et al.<sup>76</sup>. Briefly, we further partitioned the  $\beta_{ST}$  into dissimilarity due to absence of resource species (here plants) or absence of consumer species (here fungi). Moreover, we further separated interaction rewiring ( $\beta_{OS}$ ) and interaction dissimilarity ( $\beta_{WN}$ ) into "true link turnover" components and into a component due to richness dissimilarity—that is, to the inevitable difference in links due to one network being larger (having more interactions) than another<sup>6,11</sup>. To separate between these components, we used the partitioning method *com-mondenom* of the *betalinkr* function from package *bipartite* (v.2.18<sup>77</sup>). We then related the  $\beta$ -diversity of networks, and its different components, to the Euclidean distances among networks along the relevant environmental axes.

To quantify and model how the  $\beta$ -diversity of networks changes across environmental gradients, we used the analytical framework of Generalized Dissimilarity Modelling (GDM). This approach enables the nonlinear modelling of pairwise beta diversity data from differences in environmental conditions and distance between sites<sup>78</sup>. First, each predictor variable was transformed using a series of I-spline basis functions (partial regression fits). The maximum height of the predictors' I-splines was then used to characterize the proportion of ecological dissimilarity (here, network dissimilarity) explained by the predictor. The slope of the I-spline graphically indicates how the rate of ecological dissimilarity varies at any point along the gradient concerned<sup>28</sup>. Moreover, as the variables are standardized, they can be directly compared with one another, and coefficients can be calculated while holding all other variables constant<sup>78</sup>. Altogether, GDMs are known to be highly robust to multicollinearity among predictor variables<sup>33</sup>. Thus, in this context, we did not remove any of the predictor variables, and kept temperature, nitrogen and carbon content within the soil, pH, vegetation coverage and geographic distances in the final GDMs.

We fitted one GDM per network  $\beta$ -diversity component and for each site using the *gdm* package<sup>79</sup>. We used the default three I-spline basis functions for all predictors, positioned at the minimum, median and maximum of the observed values of each predictor<sup>78,79</sup>. We opted for three splines for each predictor, since this solution appears to offer a reasonable degree of flexibility in capturing nonlinear change in dissimilarities along a predictor gradient, while remaining ecologically interpretable<sup>28</sup>. Using the function "*gdm.partition.deviance*", we then applied deviance partitioning to calculate the unique and shared contributions of our set of edaphic conditions (carbon, nitrogen, and pH), temperature and vegetation coverage in explaining different components of beta diversity per site. For the edaphic conditions, the importance of each environmental predictor was estimated using the "*gdm.varImp*" function<sup>79</sup>. In applying the "*gdm.varImp*" function, the importance of each predictor is quantified as the percent change in deviance explained between a model fit with and without that predictor permuted<sup>79</sup>. However, GDMs will only permute the pairwise table, (i.e., the dissimilarity indices per pairwise comparison), but not the structure of the networks per se.

### Assessment of sample completeness

Importantly, incomplete sampling can generate "apparent turnover" between networks, where in fact there is none. This will occur when either nodes or links are actually present but not detected in the sample as due to insufficient sample size. To evaluate sample completeness, we thus drew on three considerations:

First, we based our material on a replicate sampling design: Within each of our plots, we collected three roots of three individuals per plant species, pooling all fungal records for each plot. This procedure will reduce the chance variation due to incomplete sampling of individual roots within root systems.

Second, for fungi, we carefully assessed sample coverage by inspecting taxon-accumulation curves. Should sampling be incomplete, then we expect

to encounter further taxa with further samples or sequences inspected. Nonetheless, most of our curves showed a clear asymptote well before reaching the full sample size (for detailed curves of the current material, see Parisy et al.<sup>40</sup>).

Third, we used the same rationale to assess the accumulation of new interactions with increasing sample size following Jordano<sup>80</sup> (For further details, see: Supplementary Text S2). The resulting accumulation curves are shown in Supplementary Fig. S1.1. Here, we note that sampling of interactions will always be more challenging than sampling of species<sup>38,39,81</sup>. As a result, the accumulation curves do not fully asymptote, but their shape suggests that the current sampling suffices to detect the major part of interactions.

Fourth, we used a permutation-based approach to evaluate whether the differences observed between local networks could indeed be attributed to sampling alone. For full details, see Supplementary Text 1. With respect to link turnover among shared species beyond differences in number of links (lower-right panel in Fig. 1A), observed differences were significantly larger than expected from sampling alone. With respect to compositional turnover in fungi and total dissimilarity in networks, the observed pattern was consistent with patterns expected under random sampling from a joint network (Supplementary Fig. 2). With respect to compositional turnover in fungi for the full network (i.e., the network including all fungi irrespective of functional guild), the differences detected were actually lower than expected by random sampling (Supplementary Fig. 2). In other words, the species composition of fungi was more consistent among sites than expected under random sampling from a joint species pool.

### Reporting summary

Further information on research design is available in the Nature Portfolio Reporting Summary linked to this article.

### Data availability

The raw sequences generated during the study are available in the Sequence Read Archive repository (<https://www.ncbi.nlm.nih.gov/sra>), BioProject PRJNA1178551.

### Code availability

The codes and generated datasets used for the analyses of this study are available in the Figshare open access repository at <https://figshare.com/e1da189f7ab5c804e>.

Received: 24 April 2024; Accepted: 12 November 2024;

Published online: 23 November 2024

### References

- Bahram, M. & Netherway, T. Fungi as mediators linking organisms and ecosystems. *FEMS Microbiol. Rev.* **46**, fuab058 (2021).
- Classen, A. T. et al. Direct and indirect effects of climate change on soil microbial and soil microbial-plant interactions: What lies ahead? *Ecosphere* **6**, art130 (2015).
- Poisot, T. Dissimilarity of species interaction networks: quantifying the effect of turnover and rewiring. *Peer Community J.* **2**, e35 (2022).
- Sheykhal, S. et al. Robustness to extinction and plasticity derived from mutualistic bipartite ecological networks. *Sci. Rep.* **10**, 9783 (2020).
- Vizentin-Bugoni, J., Debastiani, V. J., Bastazini, V. A. G., Maruyama, P. K. & Sperry, J. H. Including rewiring in the estimation of the robustness of mutualistic networks. *Methods Ecol. Evolution* **11**, 106–116 (2020).
- Fründ, J. Dissimilarity of species interaction networks: how to partition rewiring and species turnover components. *Ecosphere* **12**, e03653 (2021).
- Eklöf, A. & Ebenman, B. Species loss and secondary extinctions in simple and complex model communities. *J. Anim. Ecol.* **75**, 239–246 (2006).
- Nuwagaba, S., Zhang, F. & Hui, C. Robustness of rigid and adaptive networks to species loss. *PLoS ONE* **12**, e0189086 (2017).
- Robroek, B. J. M. et al. Rewiring of peatland plant–microbe networks outpaces species turnover. *Oikos* **130**, 339–353 (2021).
- CaraDonna, P. J. et al. Interaction rewiring and the rapid turnover of plant–pollinator networks. *Ecol. Lett.* **20**, 385–394 (2017).
- Noreika, N., Bartomeus, I., Winsa, M., Bommarco, R. & Öckinger, E. Pollinator foraging flexibility mediates rapid plant–pollinator network restoration in semi-natural grasslands. *Sci. Rep.* **9**, 15473 (2019).
- Zoller, L., Bennett, J. & Knight, T. M. Plant–pollinator network change across a century in the subarctic. *Nat. Ecol. Evol.* **7**, 102–112 (2023).
- Elmendorf, S. C. et al. Global assessment of experimental climate warming on tundra vegetation: heterogeneity over space and time. *Ecol. Lett.* **15**, 164–175 (2012).
- Nabe-Nielsen, J. et al. Plant community composition and species richness in the High Arctic tundra: From the present to the future. *Ecol. Evol.* **7**, 10233–10242 (2017).
- Canini, F. et al. Vegetation, pH and water content as main factors for shaping fungal richness, community composition and functional guilds distribution in soils of Western Greenland. *Front. Microbiol.* **10** (2019).
- Zhang, T., Wang, N.-F., Liu, H.-Y., Zhang, Y.-Q. & Yu, L.-Y. Soil pH is a key determinant of soil fungal community composition in the Ny-Ålesund Region, Svalbard (High Arctic). *Front. Microbiol.* **7**, 227 (2016).
- Masumoto, S. et al. Discrepancies of fungi and plants in the pattern of beta-diversity with environmental gradient imply a comprehensive community assembly rule. *FEMS Microbiol. Ecol.* **99**, fiac157 (2023).
- Poisot, T., Canard, E., Mouillot, D., Mouquet, N. & Gravel, D. The dissimilarity of species interaction networks. *Ecol. Lett.* **15**, 1353–1361 (2012).
- White, C. D., Collier, M. J. & Stout, J. C. Anthropogenic induced beta diversity in plant–pollinator networks: dissimilarity, turnover, and predictive power. *Front. Ecol. Evol.* **10** (2022).
- Post, E. et al. Ecological dynamics across the arctic associated with recent climate change. *Science* **325**, 1355–1358 (2009).
- Toju, H., Tanabe, A. S. & Sato, H. Network hubs in root-associated fungal metacommunities. *Microbiome* **6**, 116 (2018).
- Wutkowska, M., Vader, A., Mundra, S., Cooper, E. J. & Eidesen, P. B. Dead or alive; or does it really matter? level of congruency between trophic modes in total and active fungal communities in high Arctic soil. *Front. Microbiol.* **9** (2019).
- Lozano, Y. M., Aguilar-Trigueros, C. A., Roy, J. & Rillig, M. C. Drought induces shifts in soil fungal communities that can be linked to root traits across 24 plant species. *N. Phytologist* **232**, 1917–1929 (2021).
- Abrego, N. et al. Higher host plant specialization of root-associated endophytes than mycorrhizal fungi along an arctic elevational gradient. *Ecol. Evol.* **10**, 8989–9002 (2020).
- Timling, I., Walker, D. A., Nusbaum, C., Lennon, N. J. & Taylor, D. L. Rich and cold: diversity, distribution and drivers of fungal communities in patterned-ground ecosystems of the North American Arctic. *Mol. Ecol.* **23**, 3258–3272 (2014).
- Bennett, A. E. & Classen, A. T. Climate change influences mycorrhizal fungal–plant interactions, but conclusions are limited by geographical study bias. *Ecology* **101** (2020).
- Calvin, K. et al. *IPCC, 2023: Climate Change 2023: Synthesis Report. Contribution of Working Groups I, II and III to the Sixth Assessment Report of the Intergovernmental Panel on Climate Change* [Core Writing Team, H. Lee and J. Romero (Eds.)]. IPCC, Geneva, Switzerland <https://www.ipcc.ch/report/ar6/syr/> (2023).
- Mokany, K., Ware, C., Woolley, S. N. C., Ferrier, S. & Fitzpatrick, M. C. A working guide to harnessing generalized dissimilarity modelling for biodiversity analysis and conservation assessment. *Glob. Ecol. Biogeogr.* **31**, 802–821 (2022).



29. Pickett, S. T. A. in *Long-Term Studies in Ecology: Approaches and Alternatives* (ed. Likens, G. E.) 110–135 (Springer, 1989). [https://doi.org/10.1007/978-1-4615-7358-6\\_5](https://doi.org/10.1007/978-1-4615-7358-6_5).
30. Damgaard, C. A critique of the space-for-time substitution practice in community ecology. *Trends Ecol. Evol.* **34**, 416–421 (2019).
31. Myers-Smith, I. H. et al. Complexity revealed in the greening of the Arctic. *Nat. Clim. Change* **10**, 106–117 (2020).
32. Schore, A. I. G., Fraterrigo, J. M., Salmon, V. G., Yang, D. & Lara, M. J. Nitrogen fixing shrubs advance the pace of tall-shrub expansion in low-Arctic tundra. *Commun. Earth Environ.* **4**, 1–12 (2023).
33. Glassman, S. I., Wang, I. J. & Bruns, T. D. Environmental filtering by pH and soil nutrients drives community assembly in fungi at fine spatial scales. *Mol. Ecol.* **26**, 6960–6973 (2017).
34. Vázquez, D. P. et al. Species abundance and asymmetric interaction strength in ecological networks. *Oikos* **116**, 1120–1127 (2007).
35. Bonfante, P. & Anca, I.-A. Plants, Mycorrhizal fungi, and bacteria: a network of interactions. *Annu. Rev. Microbiol.* **63**, 363–383 (2009).
36. Crowther, T. W., Boddy, L. & Jones, T. H. Outcomes of fungal interactions are determined by soil invertebrate grazers. *Ecol. Lett.* **14**, 1134–1142 (2011).
37. Burkle, L. A. & Alarcón, R. The future of plant-pollinator diversity: understanding interaction networks across time, space, and global change. *Am. J. Bot.* **98**, 528–538 (2011).
38. Cirtwill, A. R., Eklöf, A., Roslin, T., Wootton, K. & Gravel, D. A quantitative framework for investigating the reliability of empirical network construction. *Methods Ecol. Evol.* **10**, 902–911 (2019).
39. Gravel, D. et al. Bringing Elton and Grinnell together: a quantitative framework to represent the biogeography of ecological interaction networks. *Ecography* **42**, 401–415 (2019).
40. Parisy, B. et al. Opportunistic partner choice among arctic plants and root-associated fungi is driven by environmental conditions. *bioRxiv* <https://doi.org/10.1101/2024.09.14.613029>.
41. Toju, H., Suzuki, S. S. & Baba, Y. G. Interaction network rewiring and species' contributions to community-scale flexibility. *PNAS Nexus* **3**, pgae047 (2024).
42. Su, M., Ma, Q. & Hui, C. Adaptive rewiring shapes structure and stability in a three-guild herbivore-plant-pollinator network. *Commun. Biol.* **7**, 1–11 (2024).
43. Batstone, R. T., Carscadden, K. A., Afkhami, M. E. & Frederickson, M. E. Using niche breadth theory to explain generalization in mutualisms. *Ecology* **99**, 1039–1050 (2018).
44. Rasmussen, P. U. et al. Elevation and plant species identity jointly shape a diverse arbuscular mycorrhizal fungal community in the High Arctic. *N. Phytologist* **236**, 671–683 (2022).
45. Zhang, T. & Yao, Y.-F. Endophytic fungal communities associated with vascular plants in the high Arctic zone are highly diverse and host-plant specific. *PLoS ONE* **10**, e0130051 (2015).
46. Wootton, K. L. et al. Layer-specific imprints of traits within a plant-herbivore-predator network—complementary insights from complementary methods. *Ecography* **2024**, e07028 (2024).
47. Bartley, T. J. et al. Food web rewiring in a changing world. *Nat. Ecol. Evol.* **3**, 345–354 (2019).
48. Cirtwill, A. R. et al. Stable pollination service in a generalist high Arctic community despite the warming climate. *Ecol. Monogr.* **93**, e1551 (2023).
49. Elkington, T. T. Studies on the variation of the genus *Dryas* in Greenland. *Medd. Om. Grønland* **178**, 1–56 (1965).
50. Philipp, M. & Siegismund, H. R. What can morphology and isozymes tell us about the history of the *Dryas integrifolia*-*octopetala* complex? *Mol. Ecol.* **12**, 2231–2242 (2003).
51. Gardes, M. & Bruns, T. D. ITS primers with enhanced specificity for basidiomycetes - application to the identification of mycorrhizae and rusts. *Mol. Ecol.* **2**, 113–118 (1993).
52. Cripps, C. L. & Eddington, L. H. Distribution of Mycorrhizal types among alpine vascular plant families on the Beartooth Plateau, Rocky Mountains, U.S.A., in reference to large-scale patterns in Arctic-Alpine habitats. *aare* **37**, 177–188 (2005).
53. Abrego, N. et al. Accounting for environmental variation in co-occurrence modelling reveals the importance of positive interactions in root-associated fungal communities. *Mol. Ecol.* **29**, 2736–2746 (2020).
54. Treu, R., Laursen, G. A., Stephenson, S. L., Landolt, J. C. & Densmore, R. Mycorrhizae from Denali National Park and Preserve, Alaska. *Mycorrhiza* **6**, 21–29 (1995).
55. Wang, B. & Qiu, Y.-L. Phylogenetic distribution and evolution of mycorrhizas in land plants. *Mycorrhiza* **16**, 299–363 (2006).
56. Koizumi, T. & Nara, K. Communities of putative Ericoid Mycorrhizal fungi isolated from Alpine Dwarf Shrubs in Japan: effects of host identity and microhabitat. *Microbes Environ.* **32**, 147–153 (2017).
57. Daghino, S., Martino, E., Voyron, S. & Perotto, S. Metabarcoding of fungal assemblages in *Vaccinium myrtillus* endosphere suggests colonization of above-ground organs by some ericoid mycorrhizal and DSE fungi. *Sci. Rep.* **12**, 11013 (2022).
58. Fujimura, K. E. & Egger, K. N. Host plant and environment influence community assembly of High Arctic root-associated fungal communities. *Fungal Ecol.* **5**, 409–418 (2012).
59. Fick, S. E. & Hijmans, R. J. WorldClim 2: new 1-km spatial resolution climate surfaces for global land areas. *Int. J. Climatol.* **37**, 4302–4315 (2017).
60. Mane, A. S., Pulugurtha, S. S., Duddu, V. R. & Godfrey, C. M. Predictor variables influencing visibility prediction based on elevation and its range for improving traffic operations and safety. *JTTs* **12**, 439–452 (2022).
61. Peña-Aguilera, P. et al. Consistent imprints of elevation, soil temperature and moisture on plant and arthropod communities across two subarctic landscapes. *Insect Conserv. Diversity* **16**, 684–700 (2023).
62. Vesterinen, E. J. et al. What you need is what you eat? Prey selection by the bat *Myotis daubentonii*. *Mol. Ecol.* **25**, 1581–1594 (2016).
63. Aljanabi, S. M. & Martinez, I. Universal and rapid salt-extraction of high quality genomic DNA for PCR-based techniques. *Nucleic Acids Res.* **25**, 4692–4693 (1997).
64. Ihrmark, K. et al. New primers to amplify the fungal ITS2 region—evaluation by 454-sequencing of artificial and natural communities. *FEMS Microbiol. Ecol.* **82**, 666–677 (2012).
65. White, B. et al. Amplification and direct sequencing of fungal ribosomal RNA Genes for phylogenetics in *PCR Protocols*. 315–322 (Academic Press, 1990).
66. Høyer, A. K. & Hodkinson, T. R. Hidden fungi: combining culture-dependent and -independent DNA barcoding reveals inter-plant variation in species richness of endophytic root fungi in *Elymus repens*. *J. Fungi (Basel)* **7**, 466 (2021).
67. Kankaanpää, T. et al. Parasitoids indicate major climate-induced shifts in arctic communities. *Glob. Change Biol.* **26**, 6276–6295 (2020).
68. Vesterinen, E. J., Puisto, A. I. E., Blomberg, A. S. & Lilley, T. M. Table for five, please: dietary partitioning in boreal bats. *Ecol. Evol.* **8**, 10914–10937 (2018).
69. Kaunisto, K. M. et al. Threats from the air: Damsel fly predation on diverse prey taxa. *J. Anim. Ecol.* **89**, 1365–1374 (2020).
70. Rognes, T., Flouri, T., Nichols, B., Quince, C. & Mahé, F. VSEARCH: a versatile open source tool for metagenomics. *PeerJ* **4**, e2584 (2016).
71. Martin, M. Cutadapt removes adapter sequences from high-throughput sequencing reads. *EMBnet. J.* **17**, 10–12 (2011).
72. Edgar, R. C. Search and clustering orders of magnitude faster than BLAST. *Bioinformatics* **26**, 2460–2461 (2010).
73. Abarenkov, K. et al. UNITE QIIME release for Fungi 2. UNITE Community <https://doi.org/10.15156/BIO/786387> (2020).
74. Nguyen, N. H. et al. FUNGuild: An open annotation tool for parsing fungal community datasets by ecological guild. *Fungal Ecol.* **20**, 241–248 (2016).



75. Novotny, V. Beta diversity of plant–insect food webs in tropical forests: a conceptual framework. *Insect Conserv. Diversity* **2**, 5–9 (2009).
76. Legendre, P. Interpreting the replacement and richness difference components of beta diversity. *Glob. Ecol. Biogeogr.* **23**, 1324–1334 (2014).
77. Dormann, C. F. Using bipartite to describe and plot two-mode networks in R. (2022).
78. Ferrier, S., Manion, G., Elith, J. & Richardson, K. Using generalized dissimilarity modelling to analyse and predict patterns of beta diversity in regional biodiversity assessment. *Diversity Distrib.* **13**, 252–264 (2007).
79. Mokany, K., Ware, C., Woolley, S. N., Ferrier, S., & Fitzpatrick, M. C. gdm: Generalized dissimilarity modeling. R package version 1.5.0-1 (2022).
80. Jordano, P. Sampling networks of ecological interactions. *Funct. Ecol.* **30**, 1883–1893 (2016).
81. Galiana, N. et al. Ecological network complexity scales with area. *Nat. Ecol. Evol.* **6**, 307–314 (2022).

## Acknowledgements

The authors are indebted to all collaborators and field assistants from the Norsk Polarinstitut; Toolik Field Station (Amanda Young); NIBIO-Svanhovd research station (Juho Vuolteenaho and Helena Klöckener), as well as to Minna Viljamaa for participating in field sampling in Finland and Norway. We are grateful to Marjo Kilpinen and Eija Takala for their help in measuring pH. We wish to acknowledge DNA analysis company Bioname for their expertise and help regarding the molecular analysis and interpretation of the sequencing results. We acknowledge CSC—IT Center for Science Ltd., Espoo, Finland, for the allocation of computational resources. We thank Pablo Peña Aguilera, Antoine Becker-Scarpitta and Giovanni Strona for stimulating discussions and early input on this study. Finally, we thank Laura Antaõ, Mariana Pires-Braga, Jussi Mäkinen, Sonja Saine, and Bess Hardwick whose comments contributed to the improvement of the manuscript. We thank the three anonymous reviewers for their valuable comments and efforts towards improving our manuscript. This research was supported by various funders of which we are thankful. BP and TR were funded by the Academy of Finland (VEGA, grant 322266 to TR). TR was also funded by the European Research Council (ERC) under the European Union’s Horizon 2020 research and innovation programme (ERC-synergy grant 856506—LIFEPLAN). BP was further supported by a grant from the Ella and Georg Ehrnrooth foundation. Field work was supported by an INTERACT Transnational and Remote Access grant (Call 2020, project VEGA). While no permissions were needed to conduct our sampling in Toolik, Ny-Ålesund, Varanger Peninsula, and Gandvik Valley, we obtained the necessary permits for sampling in Kilpisjärvi from Metsähallitus, and for sampling in Kobbefjord and Zackenberg from the Ministry of Industry, Energy, and Research, Government of Greenland.

## Author contributions

B.P., N.M.S., and T.R. designed the study. B.P., M.T., P.E.A., and T.R. collected the biological samples. C.F.C.K. and K.R. assisted in coordinating the collection of biological material. B.P. measured and produced edaphic data used in this study. Bioname, led by E.J.V, generated metabarcoding libraries from root and soil samples and produced fungal community data. B.P. analyzed the data, with input from T.R., A.R.C., H.W., N.M.S., E.V.G. B.P. and T.R. wrote the first draft of the manuscript. All authors then helped improve the manuscript or provided comments on the final manuscript.

## Competing interests

The authors declare no competing interests.

## Additional information

**Supplementary information** The online version contains supplementary material available at <https://doi.org/10.1038/s43247-024-01902-w>.

**Correspondence** and requests for materials should be addressed to Bastien Parisy.

**Peer review information** *Communications Earth & Environment* thanks Pierre-Luc Chagnon and the other, anonymous, reviewer(s) for their contribution to the peer review of this work. Primary Handling Editor: Alice Drinkwater. [A peer review file is available.]

**Reprints and permissions information** is available at <http://www.nature.com/reprints>

**Publisher’s note** Springer Nature remains neutral with regard to jurisdictional claims in published maps and institutional affiliations.

**Open Access** This article is licensed under a Creative Commons Attribution 4.0 International License, which permits use, sharing, adaptation, distribution and reproduction in any medium or format, as long as you give appropriate credit to the original author(s) and the source, provide a link to the Creative Commons licence, and indicate if changes were made. The images or other third party material in this article are included in the article’s Creative Commons licence, unless indicated otherwise in a credit line to the material. If material is not included in the article’s Creative Commons licence and your intended use is not permitted by statutory regulation or exceeds the permitted use, you will need to obtain permission directly from the copyright holder. To view a copy of this licence, visit <http://creativecommons.org/licenses/by/4.0/>.

© The Author(s) 2024